ACS Catalysis

Letter

pubs.acs.org/acscatalysis

Thiolate-Mediated Selectivity Control in Aerobic Alcohol Oxidation by Porous Carbon-Supported Au_{25} Clusters

Tatchamapan Yoskamtorn,[†] Seiji Yamazoe,[‡,§] Ryo Takahata,[‡] Jun-ichi Nishigaki,[‡] Anawat Thivasasith,[†] Jumras Limtrakul,[†,∥,⊥] and Tatsuya Tsukuda*[,‡,§]

[†]Department of Chemistry and NANOTEC Center for Nanoscale Materials Design for Green Nanotechnology, Faculty of Science, Kasetsart University, Bangkok 10900, Thailand

[‡]Department of Chemistry, School of Science, The University of Tokyo, 7-3-1 Hongo, Bunkyo-ku, Tokyo 113-0033, Japan

[§]Elements Strategy Initiative for Catalysts and Batteries (ESICB), Kyoto University, Katsura, Kyoto 615-8520, Japan

[∥]Center for Advanced Studies in Nanotechnology and Its Applications in Chemical, Food and Agricultural Industries, Kasetsart University, Bangkok 10900, Thailand

[⊥]PTT Group Frontier Research Center, PTT Public Company Limited, 555 Vibhavadi Rangsit Road, Chatuchak, Bangkok 10900, Thailand

Supporting Information

ABSTRACT: Supported Au_{25} clusters were prepared through the calcination of $Au_{25}(SC_{12}H_{25})_{18}$ on hierarchically porous carbon nanosheets under vacuum at temperatures in the range of 400−500 °C for 2−4 h. TEM and EXAFS analyses revealed that the thiolate coverage on Au_{25} gradually decreased with increasing calcination temperature and period and became negligibly small when the calcination temperature exceeded 500 °C. The catalysis of these Au_{25} clusters was studied for the aerobic oxidation of benzyl alcohol. Interestingly, the selectivity for benzaldehyde formation was remarkably improved with the increase in the amount of residual thiolates on Au_{25}, while the activity was reduced. This observation is attributed to the dual roles of the thiolates: the reduction of the oxidation ability of Au_{25} by electron withdrawal and the inhibition of the esterification reaction on the cluster surface by site isolation.

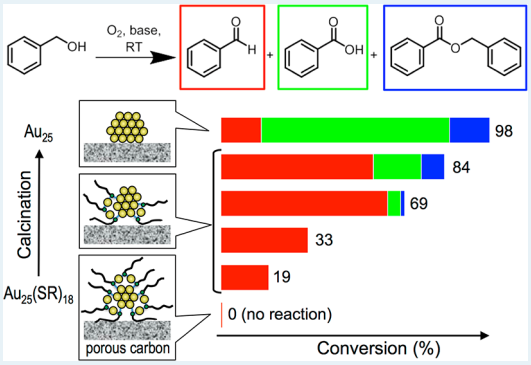

KEYWORDS: *Au_{25} clusters, carbon support, thiol, aerobic alcohol oxidation, selectivity*

INTRODUCTION

Ultrasmall (≈1 nm) metal clusters are promising candidates for novel catalytic sites owing to their unique geometrical and electronic structures. Current interest has been focused on gold clusters because they show size-specific catalysis when the diameter is smaller than 2 nm.[1−4] For an understanding of the origin of catalysis and optimization of the catalytic performance, key structural parameters such as the number of constituent atoms (cluster size) and chemical compositions must be defined with atomic precision. We and others have successfully synthesized a series of well-defined Au clusters such as Au_{11}, Au_{13}, Au_{25}, $Au_{24}Pd$, Au_{55}, and Au_{144} on solid supports by removing the thiolate (RS) or phosphine (R_3P) ligands originally acting as a protecting layer.[5−12] By using these supported catalysts, the effects of cluster size and single-atom doping on catalysis have been demonstrated.

Organic ligands on the cluster surface not only impose steric restriction on the accessibility of reactants but also modulate the electronic states of the clusters.[13] As a result, the monolayer of the ligands plays vital roles in catalysis, such as chiral modification, molecular recognition, site isolation, and charge transfer.[14−16] However, these effects will come into play at a reduced coverage because the ligands usually act as site-blocking agents or catalytic poisons. Partial removal of the ligands from $Au_{25}(SR)_{18}$ and $Au_{11}(PR_3)_7Cl_3$ makes them catalytically active for CO oxidation,[17,18] although it has been reported that Au clusters fully protected by thiolates also act as catalysts.[2,19−21] Improvement in catalytic selectivity by the ligand monolayer has been demonstrated.[22−25] These observations suggest that the chemical modification of the cluster surface is another promising approach for controlling the catalytic performance.

In this work, we study the effect of dodecanethiolates (referred to as C12S hereafter) on the catalytic activity and selectivity of Au_{25} clusters for the aerobic oxidation of benzyl alcohol. The surface coverage of C12S on Au_{25} was controlled by changing the calcination temperature and period of $Au_{25}(SC12)_{18}$. As a support, we used hierarchically porous carbon nanosheets (HPCSs) with a typical BET surface area as large as 2300 m^2/g. This porous carbon allowed us to calcine a

Received: July 16, 2014
Revised: August 30, 2014
Published: September 18, 2014

larger amount of $Au_{25}(SC12)_{18}$ than on other supports without sintering.

RESULTS AND DISCUSSION

Supported Au_{25} clusters with various coverages of C12S were synthesized as summarized briefly below.[26] First, $Au_{25}(SC12)_{18}$ and HPCSs were synthesized independently according to the reported methods.[27,28] The successful synthesis of molecularly pure $Au_{25}(SC12)_{18}$ was confirmed by UV−vis spectroscopy, matrix-assisted laser desorption ionization (MALDI) mass spectrometry, and transmission electron microscopy (TEM), as shown in Figure S1 (Supporting Information (SI)).[26,29] Scanning electron microscopy (SEM), TEM, N_2 sorption measurements, and Raman spectroscopy demonstrated that HPCSs possessed a nanosheet-aggregate structure with not only a large surface area, but also high micro- and mesoporosity (SI Figure S2).[26] Then, $Au_{25}(SC12)_{18}$ clusters were adsorbed onto HPCSs by mixing them in toluene. The $Au_{25}(SC12)_{18}$/HPCS composite collected by filtration was dried in vacuum for 4 h. The Au loading with respect to the support was determined from the optical absorbance to be 0.2 or 1.0 wt %. Finally, the composite was calcined under vacuum in the temperature range 400−500 °C for 2−4 h. Hereafter, the resulting catalysts will be referred to as $XAu_{25}(SC12)_n$/HPCS-*Y*-*Z*, where *X*, *Y*, and *Z* represent the Au loading (wt %), calcination temperature (°C), and calcination period (h), respectively.

Figure 1 shows typical TEM images of $0.2Au_{25}(SC12)_n$/HPCS-500-4 and $1.0Au_{25}(SC12)_n$/HPCS-500-4, which were

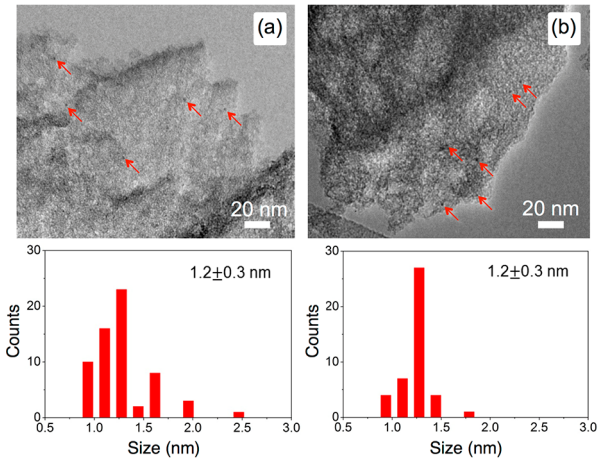

Figure 1. Typical TEM images and size distributions of Au clusters in (a) $0.2Au_{25}(SC12)_n$/HPCS-500-4 and (b) $1.0Au_{25}(SC12)_n$/HPCS-500-4.

prepared under the harshest calcination conditions employed in this work. The Au clusters were highly dispersed on the porous carbon supports. The average diameters of the Au clusters of both samples were determined to be 1.2 ± 0.3 nm, which are comparable to that of the initial $Au_{25}(SC12)_{18}$ (1.1 ± 0.3 nm). This result indicates that the aggregation of clusters is negligible even after the calcination of 1.0 wt % of $Au_{25}(SC12)_{18}$ on HPCSs at 500 °C for 4 h. Therefore, it is safe to conclude that the aggregation did not occur at the lower calciantion temperature or in the shorter calcination period. This is in sharp contrast to the results of the calcination of 1.0 wt % $Au_{25}(SC12)_{18}$ on carbon nanotubes (CNTs); they were converted to larger (>2 nm) Au nanoparticles upon calcination at 450 °C for 2 h.[10] This difference is probably due to the much larger surface area of the HPCSs (2300 m^2/g) than CNTs (200−300 m^2/g) as well as the higher population of defective sites on which the clusters can be strongly anchored or immobilized. The detailed structures of the Au clusters prepared under different calcination conditions were studied using Au L_3−edge EXAFS (Figure S5) and Fourier transformed (FT) EXAFS (Figure 2). The structural parameters obtained by

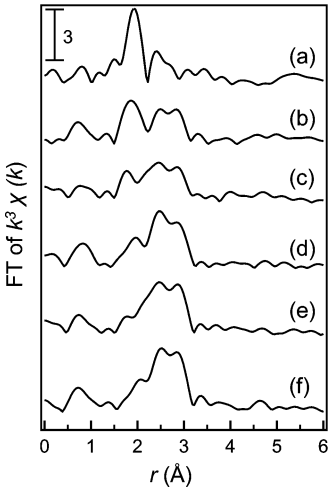

Figure 2. FT of Au L_3-edge EXAFS of (a) $1.0Au_{25}(SC12)_{18}$/HPCS and $1.0Au_{25}(SC12)_n$/HPCS-*Y*-*Z* with (*Y*, *Z*) = (400, 2), (450, 2), (450, 4), (500, 2) and (500, 4) for (b)−(f), respectively.

the curve fitting analysis of Figure 2 are listed in Table 1. Table 1 shows a gradual decrease in the coordination number (CN) values for the Au−S bonds with increasing calcination temperature and period. Calcination at 500 °C for >2 h is required for complete removal of the thiolates on HPCSs, while the thiolates are completely removed at 450 °C for 2 h on CNTs.[10] This may be due to the stronger interaction between $Au_{25}(SC12)_{18}$ and HPCSs with rough surfaces and porous frameworks than CNTs with smooth surfaces. In contrast, the CN value for the Au—Au bond before the calcination is much smaller than that expected for $Au_{25}(SC12)_{18}$ and increases with the calcination.[12] Underestimation of the CN value for the Au—Au bond in $1.0Au_{25}(SC12)_n$/HPCS has been ascribed to the fact that the Au—Au bonds in $Au_{25}(SC12)_{18}$, having multiple lengths due to various coordination environments[30] and thermal fluctuation,[31] were fitted by assuming a single length.[32] Thus, the increase in the CN value does not indicate a growth in cluster size, as demonstrated in Figure 1b, but rather an equalization of the Au—Au bond lengths during the reconstruction of the Au framework. The CN values of ≈7 after calcination at 500 °C for 4 h are reasonable for Au_{25}. Mass spectra of the desorbed species (SI Figure S3)[26] showed that the C12S ligands are desorbed mainly in the form of 1-dodecene, 1-dodecanethiol, and dodecane in the temperature range of 240−500 °C. The observation of sulfur-free species is probably due to thermal decomposition of thiols and disulfides that are desorbed from $Au_{25}(SC12)_{18}$[10] but are captured by porous carbon support.

The catalytic performances of $XAu_{25}(SC12)_n$/HPCS-*Y*-*Z* prepared under various calcination conditions were compared in the aerobic oxidation of benzyl alcohol. Table 2 summarizes the results after 6 h of the reaction. Pristine HPCSs and uncalcined composite $Au_{25}(SC12)_{18}$/HPCS did not exhibit any

dx.doi.org/10.1021/cs501010x | ACS Catal. 2014, 4, 3696−3700

Table 1. Results of Curve Fitting Analysis of Au L_3-edge EXAFS

catalyst	atom[b]	CN[c]	r (Å)[d]	$\Delta\sigma^{2e}$	R factor[f] (%)
$1.0Au_{25}(SC12)_{18}$/HPCS	S	1.6(2)	2.309(4)	0.0004(10)	14.9
	Au	0.6(3)	2.691(5)	0.0002(47)	
(1.0, 400, 2)[a]	S	0.6(1)	2.303(5)	0.0001(11)	4.9
	Au	3.1(4)	2.800(3)	0.0007(6)	
(1.0, 450, 2)[a]	S	0.4(1)	2.228(7)	0.0001(9)	8.6
	Au	6.4(9)	2.799(3)	0.0028(10)	
(1.0, 450, 4)[a]	S	0.2(1)	2.256(11)	0.0006(102)	8.2
	Au	6.4(9)	2.817(3)	0.0015(9)	
(1.0, 500, 2)[a]	Au	7.4(9)	2.796(3)	0.0022(8)	16.0
(1.0, 500, 4)[a]	Au	7.0(8)	2.805(3)	0.0015(6)	13.5

[a](*X*, *Y*, *Z*) for $XAu_{25}(SC12)_n$/HPCS-*Y*-*Z*. [b]Bonding atom. [c]Coordination number. [d]Bond length. [e]Relative Debye–Waller factor: $\Delta\sigma^2 = (\sigma_{sample}-\sigma_{reference})^2$. [f]$R$ factor = $(\Sigma(\chi^{data}-\chi^{fit})^2/\Sigma(\chi^{data})^2)^{1/2}$.

Table 2. Catalytic Performances of $XAu_{25}(SC12)_n$/HPCS-*Y*-*Z* for Aerobic Oxidation of Benzyl Alcohol[a]

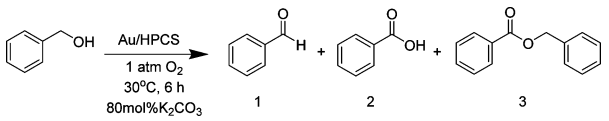

entry	catalyst	conversion (%)[d]	selectivity (%)[d] 1	2	3
1	HPCS	0	0	0	0
2	$0.2Au_{25}(SC12)_{18}$/HPCS	0	0	0	0
3	(0.2, 400, 2)[b]	3	67	33	0
4	(0.2, 450, 2)[b]	4	97	0	3
5	(0.2, 450, 4)[b]	3	98	0	2
6	(0.2, 500, 2)[b]	11	97	2	1
7	(0.2, 500, 4)[b]	84	74	21	5
8	$0.2Au_{25}$/CNT-450–2	20	40	7	53
9	(1.0, 400, 2)[b]	19	98	1	1
10	(1.0, 450, 2)[b]	33	97	1	2
11	(1.0, 450, 4)[b]	69	90	7	3
12	(1.0, 500, 2)[b]	84	67	22	11
13	(1.0, 500, 4)[b]	98	15	70	15
14	(1.0, 450, 4)[b,c]	63	95	2	3

[a]Reaction conditions: amount of catalyst: 5 mg; amount of $PhCH_2OH$: 1.2 μL; amount of K_2CO_3: 1 mg; volume of water: 1 mL; temperature: 30 °C; O_2 pressure: 1 atm; reaction time 6 h. [b](*X*, *Y*, *Z*) for $XAu_{25}(SC12)_n$/HPCS-*Y*-*Z*. [c]Recovered from Entry 11. [d]Determined by gas chromatography.

catalytic activity (Entries 1 and 2), which indicates that HPCSs are not involved in the catalysis and that a thiolate layer completely suppresses the catalyst and acts as a site-blocking reagent. The calcined $XAu_{25}(SC12)_n$/HPCS-*Y*-*Z* catalysts produced benzaldehyde (**1**), benzoic acid (**2**), and benzyl benzoate (**3**). The conversion increased gradually with increasing temperature and period of calcination at both loadings of 0.2 (Entries 3–7) and 1.0 wt % (Entries 9–13). The conversions reached 84 and 98% for $0.2Au_{25}(SC12)_n$/HPCS-500-4 (Entry 7) and $1.0Au_{25}(SC12)_n$/HPCS-500-4 (Entry 13), respectively. The calcination-induced enhancement of the catalytic activity can be ascribed to the exposure of active sites upon the removal of the thiolates. The Au_{25} clusters (1.2 ± 0.2 nm)[10] on CNTs showed higher activities than those on HPCSs under the same calcination condition (Entries 4 and 8). This is because of the easier removal of thiolates on CNTs with a smooth surface than on HPCSs with an entirely rough surface and 3D porous structure (SI Figure S2). In a recycling test (Entries 11 and 14), the conversion was reduced only slightly, but the selectivity for **1** was still high (>90%). This indicates that the catalysts are stable and can be reused.

It appears from Table 2 that there is a trade-off between selectivity and conversion. At low conversion, **1** is the major product for both loadings of 0.2 (Entries 3–6) and 1.0 wt % (Entries 9–11). In contrast, the selectivity for **1** was reduced, and those for **2** and **3** were increased at higher conversions for both loadings of 0.2 (Entry 7) and 1.0 wt % (Entries 12, 13), suggesting that the reaction proceeds sequentially.[33] In order to evaluate more rigorously the catalytic performance for the sequential reaction, we have to compare the selectivities at

Table 3. Comparison of Selectivity at Similar Conversions[a]

entry	catalyst	reaction time (h)	conversion (%)[d]	selectivity (%)[d] 1	2	3
1	(0.2, 400, 2)[b]	24	15	97	2	1
2	$0.2Au_{25}$/CNT-450–2	6	20	40	7	53
3	(1.0, 400, 2)[b]	30	37	95	1	4
4	(1.0, 450, 2)[b]	6	33	97	1	2
5	(1.0, 500, 4)[b,c]	6	32	41	18	41
6	(1.0, 450, 2)[b]	30	68	71	11	18
7	(1.0, 450, 4)[b]	6	69	90	7	3
8	(1.0, 500, 4)[b]	10 min	77	40	47	13

[a]Reaction conditions: amount of catalyst: 5 mg; amount of $PhCH_2OH$: 1.2 μL; amount of K_2CO_3: 1 mg; volume of water: 1 mL; temperature: 30 °C; O_2 pressure: 1 atm. [b](*X*, *Y*, *Z*) for $XAu_{25}(SC12)_n$/HPCS-*Y*-*Z*. [c]The amount of catalyst was reduced to 1 mg. [d]Determined by gas chromatography.

dx.doi.org/10.1021/cs501010x | ACS Catal. 2014, 4, 3696–3700

comparable conversions. Table 3 compares the selectivities of products **1**−**3** at three conversions of 15−20% (Entries 1, 2), 32−37% (Entries 3−5), and 68−77% (Entries 6−8). As expected, similar conversions were achieved in a shorter reaction time with further calcination of $1.0Au_{25}(SC12)_n$/HPCS owing to the suppression of site-blocking effects by the thiolates. The selectivity for **1** was higher with less calcination, whereas those for **2** and **3** increased significantly upon calcination. This result suggests that the residual thiolates enhance the selectivity for **1** by suppressing the oxidation reaction of **1** to **2** and the esterification reaction between **1** and **2** on the cluster surface.[23] There are two possible effects of the residual thiolates on the catalysis: steric and electronic effects. The gradual decrease of absorption threshold energies at the Au L_3-edge with the calcination temperature and period (SI Figure S4) suggests that Au_{25} clusters with the residual thiolates are more positively charged than the bare Au_{25} owing to electron withdrawal by the thiolates.[13] Thus, the suppression of oxidation of **1** to **2** is ascribed to the fact that the Au_{25} clusters are more positively charged. This trend is in parallel with the previous observation that the oxidation ability of Au clusters (1.4 nm) is significantly reduced by using less-electron-donating polymer as a stabilizer.[34] The suppression of the formation of **3** by thiolates can be explained by the site-isolation effect. This effect of thiolates has been also proposed in the oxidation of **1** over silica-supported Au nanoparticles (5.5 nm)[23] but at a low conversion (<10%). The present observation clearly demonstrates that catalytic performance of small metal clusters can be controlled through the modulation of their electronic structures and steric environments by chemical modification.

CONCLUSION

We have demonstrated herein that the coverage of dodecanethiolates (C12S) on Au_{25} plays a vital role not only in the catalytic activity but also in the selectivity for the aerobic oxidation of benzyl alcohol (BA). The Au_{25} clusters fully covered by the thiolates were inert owing to the site-blocking effect. On the contrary, thiolate-free Au_{25} clusters oxidized BA efficiently, while showing poor chemoselectivity. Interestingly, the selectivity for benzaldehyde formation was significantly improved by the presence of residual thiolates on Au_{25}, although the activity was reduced. It is proposed that the roles of thiolates are to reduce the oxidation ability of Au_{25} by electron withdrawal and to prohibit the esterification reaction on the cluster surface by site isolation. These findings demonstrate that chemical modification of the cluster surface is another important approach for controlling the catalysis of metal clusters.

EXPERIMENTAL METHODS

Preparation of Catalysts. Typical syntheses of $Au_{25}(SC12)_{18}$ and HPCSs followed previous reports.[26−28] A mixture of 100 mg HPCSs in 200 mL of toluene was sonicated for 1 h to remove impurities. The suspension was filtrated and transferred to another flask. After adding the same amount of toluene, the mixture was cooled to 0 °C and stirred for 20 min. Then, the toluene suspension of HPCSs was stirred and cooled to 0 °C for 20 min. Then, the calculated amount of $Au_{25}(SC12)_{18}$ (0.2 and 1.0 wt % Au/C) was dispersed in toluene (30 mL). The $Au_{25}(SC12)_{18}$ dispersion was injected into the HPCS suspension at the rate of 60 mL/h under vigorous stirring. After 1 h, the $Au_{25}(SC12)_{18}$/HPCS composites were filtrated and dried in vacuum for 4 h at room temperature. The dried composite in a quartz boat was subsequently placed in a furnace and calcined under vacuum with the following steps: (1) 50 °C for 30 min and (2) 400, 450, or 500 °C for 2 or 4 h. The final products were collected and kept in vials.

Catalytic Test. The aerobic oxidation of benzyl alcohol was performed under the conditions modified from refs 7 and 10. Typically, benzyl alcohol (1.2 μL, 11.6 μmol) and K_2CO_3 (1 mg) were mixed well in H_2O (1 mL) in a test tube. The mixture was then transferred to the synthesizer under vigorous stirring at 30 °C. The catalyst (5 mg) was added into the solution before purging with O_2 gas (1 atm). After the desired reaction time, the mixture was quenched with two drops of 2 M aqueous HCl solution and extracted with toluene. The obtained organic layer was analyzed with a gas chromatograph with a frame ionization detector by using an external standard method. The entire mass balance was greater than or equal to 95%. The conversion of benzyl alcohol is defined as the percentage of the total amount of benzyl alcohol consumed in the oxidation reaction to the total amount of benzyl alcohol at the initial time. The selectivity of the reaction is denoted as the ratio of benzyl alcohol converted to the corresponding products.

ASSOCIATED CONTENT

Supporting Information

Details of experimental procedures and characterization results. This material is available free of charge via the Internet at http://pubs.acs.org.

AUTHOR INFORMATION

Corresponding Author

*E-mail: tsukuda@chem.s.u-tokyo.ac.jp.

Notes

The authors declare no competing financial interest.

ACKNOWLEDGMENTS

We thank Prof. Hiroshi Nishihara (The University of Tokyo) for allowing us to access the TEM apparatus. This research was supported financially by the Funding Program for Next Generation World-leading Researchers (NEXT Program, GR-003) and "Elements Strategy Initiative for Catalysts & Batteries (ESICB)". T.Y. thanks the Development and Promotion of Science and Technology Talents Project (DPST) from the Ministry of Science and Technology, the Ministry of Education, and the Institute for the Promotion of Teaching Science and Technology (IPST) of Thailand. This work was partially supported by grants from the National Science and Technology Development Agency (NANOTEC Center for Nanoscale Materials Design for Green Nanotechnology funded by the National Nanotechnology Center), the Commission on Higher Education, Ministry of Education (the "National Research University Project of Thailand (NRU)", and the "National Center of Excellence for Petroleum, Petrochemical and Advanced Materials (NCE-PPAM)").

REFERENCES

(1) Tsukuda, T.; Tsunoyama, H.; Sakurai, H. *Chem.—Asian J.* **2011**, *6*, 736−748.
(2) Li, G.; Jin, R. C. *Acc. Chem. Res.* **2013**, *46*, 1749−1758.
(3) Yamazoe, S.; Koyasu, K.; Tsukuda, T. *Acc. Chem. Res.* **2014**, *47*, 816−824.

(4) Taketoshi, A.; Haruta, M. *Chem. Lett.* **2014**, *43*, 380−387.
(5) Menard, L. D.; Xu, F. T.; Nuzzo, R. G.; Yang, J. C. *J. Catal.* **2006**, *243*, 64−73.
(6) Turner, M.; Golovko, V. B.; Vaughan, O. P. H.; Abdulkin, P.; Berenguer-Murcia, A.; Tikhov, M. S.; Johnson, B. F. G.; Lambert, R. M. *Nature* **2008**, *454*, 981−983.
(7) Liu, Y.; Tsunoyama, H.; Akita, T.; Tsukuda, T. *J. Phys. Chem. C* **2009**, *113*, 13457−13461.
(8) Liu, T.; Tsunoyama, H.; Akita, T.; Tsukuda, T. *Chem. Commun.* **2010**, *46*, 550−552.
(9) Liu, Y.; Tsunoyama, H.; Akita, T.; Xie, S.; Tsukuda, T. *ACS Catal.* **2011**, *1*, 2−6.
(10) Xie, S.; Tsunoyama, H.; Kurashige, W.; Negishi, Y.; Tsukuda, T. *ACS Catal.* **2012**, *2*, 1519−1523.
(11) Ma, G. C.; Binder, A.; Chi, M. F.; Liu, C.; Jin, R. C.; Jiang, D. E.; Fan, J.; Dai, S. *Chem. Commun.* **2012**, *48*, 11413−11415.
(12) Shivhare, A.; Chevrier, D. M.; Purves, R. W.; Scott, R. W. J. *J. Phys. Chem. C* **2013**, *117*, 20007−20016.
(13) Walter, M.; Akola, J.; Lopez-Acevedo, O.; Jadzinsky, P. D.; Calero, G.; Ackerson, C. J.; Whetten, R. L.; Grönbeck, H.; Häkkinen, H. *Proc. Natl. Acad. Sci. U.S.A.* **2008**, *105*, 9157−9162.
(14) Mallat, T.; Orglmeister, E.; Baiker, A. *Chem. Rev.* **2007**, *107*, 4863.
(15) Schoenbaum, C. A.; Schwartz, D. K.; Medlin, J. W. *Acc. Chem. Res.* **2014**, *47*, 1438−1445.
(16) Niu, Z.; Li, Y. *Chem. Mater.* **2014**, *26*, 72−83.
(17) Wu, Z.; Jiang, D.; Mann, A. K. P.; Mullins, D. R.; Qiao, Z. A.; Allard, F. L.; Zeng, C.; Jin, R.; Overbury, S. H. *J. Am. Chem. Soc.* **2014**, *136*, 6111−6122.
(18) Lopez-Acevedo, O.; Kacprzak, K. A.; Akola, J.; Häkkinen, H. *Nat. Chem.* **2010**, *2*, 329−334.
(19) Qian, H.; Zhu, M.; Jin, R. C. *Acc. Chem. Res.* **2012**, *45*, 1470.
(20) Nie, X. T.; Zeng, C. J.; Ma, X. G.; Qian, H. F.; Ge, Q. J.; Xu, H. Y.; Jin, R. C. *Nanoscale* **2013**, *5*, 5912−5918.
(21) Nie, X. T.; Qian, H. F.; Ge, Q. J.; Xu, H. Y.; Jin, R. C. *ACS Nano* **2012**, *6*, 6014−6022.
(22) Haider, P.; Urakawa, A.; Schmidt, E.; Baiker, A. *J. Mol. Catal. A: Chem.* **2009**, *305*, 161−169.
(23) Chen, K.; Wu, H.; Hua, Q.; Chang, S.; Huang, W. *Phys. Chem. Chem. Phys.* **2013**, *15*, 2273−2277.
(24) Marshall, S. T.; O'Brien, M.; Oetter, B.; Corpuz, A.; Richards, R. M.; Schwartz, D. K.; Medlin, J. W. *Nat. Mater.* **2010**, *9*, 853−858.
(25) Kwon, S. G.; Krylova, G.; Sumer, A.; Schwartz, M. M.; Bunel, E. E.; Marshall, C. L.; Chattopadhyay, S.; Lee, B.; Jellinek, J.; Shevchenko, E. *Nano Lett.* **2012**, *12*, 5382−5388.
(26) See the Supporting Information.
(27) Qian, H. F.; Liu, C.; Jin, R. C. *Sci. China Chem.* **2012**, *55*, 2359−2365.
(28) Ma, M.; Zacher, D.; Zhang, X.; Fischer, R. A.; Metzler-Nolte, N. *Cryst. Growth Des.* **2011**, *11*, 185−189.
(29) Zhu, M. Z.; Eckenhoff, W. T.; Pintauer, T.; Jin, R. C. *J. Phys. Chem. C* **2008**, *112*, 14221−14224.
(30) MacDonald, M. A.; Chevrier, D. M.; Zhang, P. *J. Phys. Chem. C* **2008**, *112*, 15282−15287.
(31) Devadas, M. S.; Bairu, S.; Qian, H.; Sinn, E.; Jin, R.; Ramakrishna, G. *J. Phys. Chem. Lett.* **2011**, *2*, 2752−2758.
(32) Simms, G. A.; Padmos, J. D.; Zhang, P. *J. Chem. Phys.* **2009**, *131*, 214703−214709.
(33) Wang, S.; Zhao, Q.; Wei, H.; Wang, Z.-Q.; Cho, M.; Cho, H. S.; Terasaki, O.; Wan, Y. *J. Am. Chem. Soc.* **2013**, *135*, 11849−11860.
(34) Tsunoyama, H.; Ichikuni, N.; Sakurai, H.; Tsukuda, T. *J. Am. Chem. Soc.* **2009**, *131*, 7086−7093.